

Kazakhstan's crude oil contains significant amounts of heavy hydrocarbons that solidify as wax at lower temperatures, leading to reduced flow rates and potential blockages in pipelines. Paraffin, a substantial component of crude oil, crystallizes below its pour point, posing challenges for maintaining efficient crude oil transportation. Addressing wax deposition is essential for optimizing oil flow and meeting global energy demand. This article presents an innovative method for forecasting paraffin deposition in Kazakh crude oil, using its chemical composition and thermobaric conditions. The methodology encompassed data analysis, ASTM-standard laboratory tests, and computations employing modified equations for fusion properties calculation. Outcomes comprise computed temperatures, enthalpy, and heat capacity related to melting, along with revised correlations for melting and pour points specific to Kazakh crude oils. The melting point correlation was modified to fit the properties of Kazakh crude oils, resulting in standard deviation of 0.55 %. Computed pour points for hydrocarbons improved by 17 % respectively. As a result of the research a novel software tool was developed and evaluated, highlighting the project's contribution in providing an adjusted thermodynamic model for paraffin deposition forecasting. Comparisons between the developed software, PVTsim, and field data showed the wax appearance temperature (WAT) predictions closely aligned, with 0.74 % of error. This numerical tool shows potential in predicting wax deposition, thus aiding in the planning of oil production and refining processes in Kazakhstan. The importance of this work extends to its potential economic impact on companies and the nation, as well as its environmental benefits by facilitating eco-friendly planning of oil production facilities. Future research could expand on these findings to further enhance predictive models of paraffin precipitation across diverse conditions

Keywords: forecasted model, paraffin deposition, pour point, melting point, PVT, multisolid model

DEVELOPMENT OF PREDICTIVE MODEL FOR DETERMINATION OF PARAFFIN DEPOSITION IN KAZAKH CRUDE OIL

Adel Sarsenova

Corresponding author

Master of Science in Petroleum Engineering, Senior Lecturer*

E-mail: adel.askarbekovna@gmail.com

Jamilyam Ismailova

PhD, Associate Professor**

Abdulakhat Ismailov

PhD, Candidate of Technical Sciences, Professor*

Dinara Delikesheva

Master of Technical Sciences, Senior Lecturer**

Aigerim Kaidar

Master of Science in Petroleum Engineering**

*School of Energy and Petroleum Industry

Kazakh-British Technical University

Tole-bi str., 59, Almaty, Republic of Kazakhstan, 050000

**Department of Petroleum Engineering

Satbayev University

Satbayev str., 22, Almaty, Republic of Kazakhstan, 050013

Received date 18.03.2024

Accepted date 06.06.2024

Published date 28.06.2024

How to Cite: Sarsenova, A., Ismailova, J., Ismailov, A., Delikesheva, D., Kaidar, A. (2024). Development of predictive model for determination of paraffin deposition in Kazakh crude oil. *Eastern-European Journal of Enterprise Technologies*, 3 (8 (129)), 21–35.

<https://doi.org/10.15587/1729-4061.2024.306971>

1. Introduction

A significant portion of Kazakhstan's crude oil comprises heavy hydrocarbons that tend to precipitate as wax solids at lower temperatures. Paraffin, being a substantial component of crude oil, solidifies below its pour point. The accumulation of deposited paraffin on pipeline walls presents a complex challenge in maintaining flow, leading to reduced flow rates and potential blockages by narrowing the cross-sectional flow area in pipelines. Moreover, above-ground facilities experience heightened energy consumption and equipment malfunctions caused by wax blockages. The deposition of wax further escalates the oil mixture's viscosity, consequently raising the energy demand for crude oil transportation.

Understanding and addressing the issue of wax deposition in pipelines is critical for several reasons. Firstly, as the global demand for energy continues to rise, ensuring the efficient transportation of crude oil is paramount to meeting this demand. Any disruptions caused by wax blockages can lead to significant economic losses and energy inefficiencies. For in-

stance, the oil and gas industry incurs billions of dollars annually in maintenance and production losses due to wax-related issues. Secondly, the extraction and transportation of crude oil from regions with colder climates, such as Kazakhstan, are particularly susceptible to wax deposition problems, making it essential to develop effective mitigation strategies. Given the significant reserves of heavy oil in these regions, tackling wax deposition is crucial for optimizing resource utilization.

Moreover, with the ongoing advancements in deep-water and arctic oil extraction, the industry faces even more severe challenges related to wax deposition due to the extremely low temperatures in these environments. These frontier areas are becoming increasingly important as conventional oil reserves dwindle, and ensuring the flow assurance in such harsh conditions is vital for the future of oil exploration and production. Consequently, research in this area remains highly relevant, as the development of new technologies and methods to predict and control wax formation can significantly enhance the operational efficiency and safety of oil transportation systems.

Several methodologies have emerged within the realms of science and industry to forecast and mitigate flow assurance issues. A prevalent approach involves predicting the wax appearance temperature (WAT), which considers the temperature-dependent solubility parameters of individual components in both liquid and solid phases, alongside their molar volumes. Accurate prediction of WAT is essential for designing and operating pipelines and processing facilities in a cost-effective manner. Currently, two types of models are utilized for wax deposition calculations. One model posits that the precipitated wax forms a solid solution, while the other assumes that the separated phase comprises multiple solid phases.

Given these points, it is evident that research devoted to the development of more accurate predictive models and effective mitigation techniques for wax deposition is highly relevant. The ongoing challenges in both established and emerging oil production areas necessitate continuous improvement in our understanding and handling of wax-related flow assurance issues. Therefore, it is essential to explore and understand the existing achievements in this field, identify gaps in current knowledge, and drive further advancements to address this persistent challenge in the oil industry.

2. Literature review and problem statement

Petroleum reservoir fluids are intricate blends of hydrocarbons, with detailed knowledge of their composition and properties remaining elusive. The lighter fraction of these fluids comprises associated gases and low-molecular-weight hydrocarbons like CO_2 , H_2S , N_2 , CH_4 , C_2H_6 , C_3H_8 , $n\text{-C}_4\text{H}_{10}$, and $i\text{-C}_4\text{H}_{10}$. On the other hand, the bulk of the oil contains substantial quantities of paraffinic hydrocarbons, naphthenic compounds, and aromatic compounds, with molecular weights ranging from around 100 to 2000 [1]. As temperatures decrease, heavy hydrocarbon components within this molecular weight range can undergo crystallization, forming solid masses known as wax. These wax deposits can accumulate on the walls of the wellbore, thereby reducing its effective flow area on pipe walls or process equipment [2]. Additionally, it can also degrade the rheological characteristics waxy oil, potentially resulting in blockages within the wellbore [3] leading to operational and economic repercussions that are highly significant to the petroleum industry [4]. The molecular and thermodynamic characteristics of the lighter fraction of petroleum fluids are well-understood and accurately known. However, the situation is considerably different for the heavier hydrocarbon fractions. Their complexity and the fact that their properties vary depending on the crude oil make their generalized behavior challenging to comprehend and predict. Despite these challenges, substantial experimental data and simplified modeling descriptors have been published over the past few years.

The effective design of oil recovery processes necessitates accurate prediction of the thermodynamic conditions leading to wax precipitation from crude oil. This prediction depends on factors such as pressure, temperature, and oil composition. Over time, various thermodynamic models have been proposed in the literature, utilizing activity coefficients and/or equations of state (EOS). These models are employed to calculate the solubility of heavy hydrocarbons in both synthetic and real petroleum fluids under varying pressures, ranging from low to high. The proposed models

vary in how they formulate equilibrium relationships for the resulting solid phase. However, a common parameter among these models is the assessment of the fugacity of solid phase components. The handling of this parameter varies across different applications and contexts, highlighting the diversity and complexity of thermodynamic modeling in the field of petroleum engineering [5].

According to [6] models for wax precipitation have been developed using two distinct approaches. One approach is employing cubic EOS for vapor-liquid equilibrium and activity coefficient for solid – liquid equilibrium for wax precipitation modeling, while another involves applying only EOS for all phases in equilibrium.

The paper [7] initially developed a model in 1986 to predict wax precipitation in condensate oil using solid solution theory. They employed the SRK equation and modified regular solution theory to account for the non-ideal behavior of the liquid phase. However, the inconsistency in thermodynamics in their approach limited its predictive capability.

Another model for wax precipitation was proposed by [8], assuming wax to consist of multiple phases, each described separately as a pure component. They experimentally measured wax crystal formation from a condensate mixture of six alkanes, finding good agreement between predicted and experimental solid content trends with temperature. The authors employed the Peng-Robinson equation of state to calculate component fugacity in liquid phases and adjusted the melting point proposed by [7]. They also modified the enthalpy of fusion for paraffinic hydrocarbons due to overestimation below the cloud point. Experimental and analytical work on binary and multicomponent mixtures demonstrated improved results, leading to widespread adoption of the model in the field. However, [9] later demonstrated limitations in the applicability of this model, showing significant fluctuations in results when physical parameters of oil samples varied.

In the research [9] multiple solid-phase model initially proposed by [8] was refined. This refinement involved categorizing each heavy fraction into paraffins, naphthenes, and aromatic hydrocarbons. This refinement enhanced the model's accuracy by better representing the components contributing to wax formation. It was identified that cloud point temperature (CPT) can decrease significantly with increasing pressure and the presence of light hydrocarbons, demonstrating composition effect. The study highlighted the significant impact of pressure on CPT and wax precipitation. However, the model had some drawbacks in accounting for the influence of solid-phase composition and pressure on solid phase non-ideality.

Furthermore, it should be mentioned that most literature-based methods for predicting crystallization temperature [7–11] rely on thermodynamic phase equilibrium relationships. For instance, [9] presented methods to predict cloud point temperatures and quantify wax precipitation in crude oils. Similarly, [7, 8] explored the thermodynamic principles governing solid-liquid-vapor in heavy hydrocarbon mixtures, focusing on wax formation as well. [11] integrated Flory's polymer solution theory and the concept of metastable subcooled states, providing a robust theoretical framework for understanding wax formation in crude oils. Additionally, [9] investigated crystallization and dissolution temperatures of North Sea crude oils. Utilizing polarization microscopy, differential scanning calorimetry (DSC), and viscometry, this research characterized seventeen crude

oils and condensates. The study revealed that polarization microscopy provides the highest wax precipitation temperatures (WPT), essential for predicting wax deposition onset. It also highlighted the significant impact of thermal history on viscosity and pour point, with reheating and cooling cycles markedly altering these properties. Compositional analysis indicated that wax precipitating just below the WPT is richer in condensed naphthenes and poorer in isoalkanes. These methods adjust the fugacity and its coefficient as primary parameters to forecast crystallization points and wax deposition amounts. In essence, adjusting these thermodynamic parameters predicts deposition points and wax quantities. The common methodology used in these models is based on solid solution theory, which posits that the precipitated wax forms a single solid phase in which all components are fully dissolved into each other.

Thermodynamic models are formulated using intricate properties like interaction coefficients, critical properties, acentric factor, solubility parameters, and molecular weight. These models do not specifically account for long-chain waxes found in crude oil. To create a thermodynamic model capable of accurately describing wax phase behavior in crude oils, a robust approach is essential. The perturbed-chain statistical associating fluid theory (PC-SAFT) equation of state proves particularly valuable for simulating the phase behavior of complex structures such as waxes within crude oil. In the study [5], a new methodology was introduced that utilizes the wax appearance temperature of crude oil to predict and determine the necessary PC-SAFT parameters for accurately simulating wax crystallization in crude oil. Additional research [12, 13] applies the PC-SAFT equation of state to model the behavior of the liquid phase and uses a multi-solid framework to describe the solid phase, aiding in the prediction of wax deposition. Despite the advances of these models there are still critical areas that require further investigation. For instance:

[14] demonstrated that the perturbed-chain statistical associating fluid theory (PC-SAFT) model could correlate wax precipitation better than basic models, but it did not address the specific onset of precipitation temperatures;

[15] introduced a method for estimating effective parameters to predict precipitation behavior more accurately, yet it still faces challenges in representing the exact temperature at which each component precipitates.

One of the recent advances is prediction of wax deposition by using Aspen HYSYS software [16]. However, it falls short in estimation of wax appearance temperature (WAT) and wax precipitation curve. Study [17] shows open-source software (SP-Wax) to calculate the solid-liquid equilibrium of wax in a mixture of wax hydrocarbons. It allowed more accurate prediction of solid phase composition than others. All this suggests that it is advisable to address the issues of inaccurate paraffin deposition predictions.

Despite advancements in wax deposition modeling, the current progress is considered modest, since the results from these models in predicting wax formation often do not align closely with experimental data due to its insufficiency and tend to overestimate the amount of precipitated wax and the cloud temperatures of oil. Ideal solution models, when suitably adjusted, can offer qualitative descriptions across a wide pressure and temperature range.

The proposed modification of the thermodynamic paraffin forecasting model and the planned development of correlations represent the sole analytical solution for predicting

the crystallization temperature of paraffin (or mixtures of heavy paraffin hydrocarbons) in specific Kazakhstan oils.

This correlation relies on the intensive properties of the solution components, such as their molecular weights and melting points, as well as external properties like mass fractions [18]. In simpler terms, the independent variables include the solute's weight fraction, molecular weight, melting point temperature, and the solution's molecular weight.

3. The aim and objectives of the study

The aim of this study is to develop an innovative approach for forecasting paraffin deposition in Kazakh crude oil by leveraging its chemical composition and thermobaric conditions. This will make it possible to predict and mitigate issues related to wax formation, ensuring smoother operations and reduced maintenance costs in oil extraction and transportation processes.

To achieve this aim, the following objectives are accomplished:

- to calculate enthalpy and heat capacity of fusion;
- to determine melting, freezing points and their modifications;
- to calculate pour point for mixture;
- to formulate and implement the “Multisolid” paraffin model;
- to conduct numerical simulations using the developed thermodynamic model.

4. Materials and methods

4.1. Object and hypothesis of the study

The object of the study is wax precipitation in Kazakh crude oil. The subject of the study is addressing the challenges of computing properties related to wax deposition.

The methodology of this work incorporated theoretical, experimental, and computational approaches. It was conducted in collaboration with “StratumCER” LLP, utilizing standard laboratory equipment and instrumentation to analyze physical and chemical properties of surface oil samples. These instruments underwent metrological verification in 2020 (Accreditation Certificate No.). The theoretical framework involved the modification of existing equations for fusion properties, specifically tailored to Kazakh crude oils. Theoretical calculations were performed to determine critical properties such as melting temperatures, enthalpy, and heat capacity. These modified equations and calculations formed the backbone of the predictive model.

4.2. Collecting and analyzing field data from X and Y fields

During the execution of this task, data provided by an interested company was collected and meticulously analyzed. The process involved several key steps:

- a comprehensive critical analysis of scientific research literature and publications concerning methods for calculating models of multicomponent mixtures to predict paraffin precipitation. This analysis led to the determination of a calculation algorithm based on the methodology proposed in [8].
- oil samples were procured from two fields specifically for further research purposes;

- the components of the C₁-C₆ and C₇₊ fractions were characterized based on the data obtained from the report;
- critical parameters for each hydrocarbon component were calculated using the data acquired during the analysis process;
- PVT reports from 66 wells, which are essential for subsequent calculations, were collected and thoroughly analyzed.

4. 3. Calculating melting properties related to wax deposition

4. 3. 1. Calculations of enthalpy and heat capacity of fusion

Melting enthalpy: Δh_i^f .

The melting enthalpy refers to the quantity of heat required to convert one unit of mass of a crystalline substance from a solid state to a liquid state in an equilibrium isobaric-isothermal process. Conversely, the same amount of heat is released when the substance undergoes crystallization from a liquid to a solid state.

In this work, the enthalpy of the substance was calculated using formula in [9]:

$$\Delta h_i^f = 0.05276 M_i T_i^f \Delta h_i^f = 0.05276 M_i T_i^f. \quad (1)$$

The constant 0.05276 represents the average slope when the entropy of melting $\left(\frac{\Delta h_i^f}{T_i^f}\right)$ presented as a function of the molecular weight of paraffinic hydrocarbons.

4. 3. 2. Enthalpy of transition to solid state

The enthalpy of transition to a solid state refers to the process in which a substance transitions from state *A* to state *B*, specifically from a liquid to a solid state. It is a thermodynamic term that quantifies the amount of heat released during this transition between states. Conventionally, the positive heat release during this transition is considered numerically equal to the negative enthalpy change. Based on this concept, the enthalpy of combustion and the enthalpy of evaporation have numerically equal values because they represent different processes where heat is either released (enthalpy of combustion) or absorbed (enthalpy of evaporation) but are equal in magnitude.

In this work, the enthalpy of a substance was calculated using [19]:

$$\Delta h_i^r = 0.05776 M_i T_i^f. \quad (2)$$

This equation relates the transition enthalpy of a substance to its molar mass and melting point temperature. It calculates the energy changes associated with phase transition of wax components, which is crucial for accurate modeling and prediction of wax deposition.

4. 3. 3. Heat capacity of fusion

The heat capacity of fusion is a property that quantifies the amount of thermal energy needed to raise the temperature of a specific system. Experimental observations indicate that the heat transferred in this process depends on three key factors: (1) temperature changes, (2) the mass of the system, and (3) the substance and its phase. Typically, heat capacity of fusion is expressed in calories per degree per mole, where the mole represents the actual amount of material in question (often measured in grams, corresponding to the molecular weight).

In this work, the heat capacity of fusion is calculated using the formula in [9]:

$$\Delta C_{pi} = 0.3033 M_i - 4.635 * 10^{-4} M_i T_i^f. \quad (3)$$

The equation relates the change in heat capacity at constant pressure of a substance to its molar mass and the square of its melting point temperature. The presence of these two terms suggests that the change in heat capacity is influenced by both the intrinsic properties of the substance (molar mass) and the thermal conditions (melting point temperature).

4. 4. Melting, freezing points and their modifications

4. 4. 1. Melting temperature, T_i^f

The melting point refers to the temperature at which a crystalline solid transition into a liquid state. At this point, the substance can exist in either a liquid or solid form. In this project, correlation proposed in [7] was adapted and modified to calculate the melting point of alkanes. This correlation, chosen for its widespread acceptance, uses the molecular weights of individual components to determine their respective melting points:

$$T_i^f = 374.5 + 0.02617 * M_i - \frac{20172}{M_i}. \quad (4)$$

Here is the algorithm for performing correlation modification as described:

1. Utilize the experimental results to calculate the melting temperatures of each component.
2. Develop a program using the Python programming language (refer to Appendix K) to determine correlation coefficients, aiming to enhance the accuracy of the calculations.
3. Conduct a test of the calculation results using the modified correlation to validate its effectiveness and accuracy.

Thus, the modified correlation [20] for the Kazakhstan X field is as follows:

$$T_i^f = 101.82154 + 0.02617 * M_i - 20172 / M_i. \quad (5)$$

The dependence of the melting temperature T_m on the molecular weight of the component M_{wi} is presented in the graph below for components from hexane C₆ to hexatriacontane C₃₆₊ for the Uzen field. The absolute mean deviation was calculated for these components using the following formula:

$$MAD = \frac{1}{n} \sum_{i=1}^n |x_i - m(X)|. \quad (6)$$

Further, according to the article [6], experimental findings indicated that only heavy hydrocarbons, specifically those from C₁₅ to C₂₀ and beyond, are present in precipitated paraffin. To enhance the accuracy of the results for the components ranging from pentadecane C₁₅H₃₂ to eicosane C₂₀H₄₂, the correlation was recalculated using the Python programming language. The equation captures a balance between the linear increase and inverse decrease in temperature as a function of molecular weight:

$$T_i^f = 99.833 + 0.02617 * M_i - 20172 / M_i. \quad (7)$$

A graph was generated, showing an 11 % improvement in accuracy for these six components compared to the [7] correlation.

4. 4. 2. Temperature of solid-state transition (solidification)

The pour point is the lowest temperature at which oil, petroleum products, or lubricating oil remains mobile and flows as a liquid. This temperature is influenced by the presence and amount of paraffin in the oil or petroleum product. As part of this project, a modification was made to the [20] to determine the solid-state transition temperature, specifically the solidification temperature, of alkanes. [14] modified the equation as follows:

$$T_{ii}^{tr} = 366.39775 + 0.003609M_i - \frac{20879.6}{M_i}. \quad (8)$$

Below is an algorithm for performing correlation modification:

1. Utilize the data from experiments to calculate the pour point results for each component.

2. Develop a program using the Python programming language to determine correlation coefficients, aiming to enhance the accuracy of the calculations.

3. Conduct a test of the calculation results using the modified correlation to validate its effectiveness and accuracy.

Final correlation value:

$$T_{ii}^{tr} = 95.666 + 0.003609M_i - \frac{20879.6}{M_i}. \quad (9)$$

As can be seen in (9) the values of the constants A, B, and C were changed to improve the correlation's accuracy. By modifying these constants, the goal was to refine the predictive capability of the correlation equation, thereby providing more accurate pour point results for different components.

4. 4. 3. Melting point for mixture

The molecular weight of the mixture was calculated in two steps, the first for components C₃ to C₆, and the second for components C₇₊. The molecular weights of components C₃ to C₆ were calculated using Kay's mixing rules:

$$M_{wi} = \sum_{i=1}^n m_i M_i. \quad (10)$$

The molecular weight of components from C₇₊ was calculated using the rules of exponential distribution, namely the Lorenz-Bray-Clark correlation:

$$M_{C_{n+}} = \sum_{i=n}^{\infty} z_i M_i / z_{C_{n+}}. \quad (11)$$

The calculation results for deposits X and Y are presented in the Table 5.

Using the molecular weight values obtained, calculate the melting temperature for the X field using the [6] correlation. Consequently, the modified correlation specific to the Kazakhstan X field can be expressed as follows [20]:

$$T_i^f = 102.333 + 0.02617 * M_i - 20172 / M_i. \quad (12)$$

This equation expresses the melting point temperature of a component as a function of its molar mass. It shows that the melting point temperature is influenced by both the magnitude and the reciprocal of the molar mass. For components with higher molar masses, the linear term

dominates, leading to an overall increase in melting point. For components with lower molar masses, the inverse term has a larger impact, potentially lowering the melting point.

4. 4. 5. Pour point for mixture.

For calculating pour point for mixtures Python programming language was utilized. The final correlation value is shown below [20]:

Final correlation value:

$$T_{ii}^{tr} = 71.3333 + 0.003609M_i - \frac{20879.6}{M_i}. \quad (13)$$

The proposed correlation for measuring the pour point showed a 7 % improvement in efficiency compared to [9].

4. 5. Formulating and implementing the "Multisolid" paraffin model

Model and calculation method statement:

1. Begin.
2. Enter initial data, including molecular weight, mole percentage, or raw PNA analysis (paraffins, naphthenes, aromatics), and specify temperature (T) and pressure (P).
3. Subroutine 1: evaluate component properties.
4. Subroutine 2: assess the necessary properties for calculating the fugacity coefficient.
5. Subroutine 3: calculate fugacity using the equation of state.
6. Subroutine 4: analyze phase stability.
7. Estimate initial values for deposited components in vapor and liquid phases.
8. Subroutine 5: perform flash calculation.
9. End.

The algorithm for solving the multi-solid-phase model comprises five subroutines:

- subroutine 1: calculate component properties (such as T_C , P_C , w , etc.) using a dedicated calculation program;
- subroutine 2: estimate parameters (T_{if} , h_{if} , CP_i) necessary for calculating the fugacity coefficient using a computer program;
- subroutine 3: calculate the fugacity of each component in both liquid and vapor phases, considering pure components and mixtures;
- subroutine 4: determine the number and nature of precipitating components in the pure solid phase under various temperature and pressure conditions. This subroutine conducts phase stability analysis for all components;
- subroutine 5: perform main calculations using a specific flash type calculation program. The Multisolid model relies on the precipitation of specific heavy components within crude oil, with average properties assigned to each fraction.

At the onset of deposition, an unstable solid solution emerges wherein the components are temporarily mixed in varying proportions. However, after a characteristic duration, the spontaneous separation of this solid solution results in a final stable state comprising pure hydrocarbon components. In other words, the precipitated paraffin forms a mass of pure hydrocarbon components containing the precipitating components, which are immiscible with each other.

The amount of precipitated paraffin as a percentage of the oil is calculated as:

$$\text{wax wt \% in oil} = 100 \times \frac{\sum_{i=1}^N M_i n_i^s}{F \sum_{i=1}^N z_i M_i}, \tag{14}$$

where M – total number of moles of original oil and number of moles of component i precipitated as a solid; M_i – molecular weight of the component i ; z_i – its mole fraction in the original liquid.

As with any laboratory and analytical research, there is an error.

Deviation assessment:

$$AAD(\%) = \frac{100 \sum_{i=1}^{i=n} |WAP_{expi} - WAP_{cali}|}{n WAP_{expi}}, \tag{15}$$

AAD – absolute average deviation (%);

WAP – wax appearance point (K).

Based on the existing stability criteria: any component (i) can exist as a pure solid if:

$$f_i(P, T, z) - f_{purei}^s(P, T) \geq 0, \quad (i = 1, 2, \dots, N), \tag{16}$$

where fugacity component i for a given composition z represented. At fixed temperature and pressure for any component i , in the multisolid phase model, the following conditions hold at equilibrium.

The activity coefficient of component i in the mixture is equal to the fugacity of component in the mixture.

The fugacity of component i in the mixture is equal to the fugacity of component in its pure state.

In other words, at equilibrium, the fugacity of each component in the mixture is equal to the fugacity of the same component when it is in its pure form. This condition must be satisfied for all components in the model (where i ranges from 1 to N , with N being the total number of components).

This implies that the behavior of each component in the mixture can be described as if it were in its pure state, which simplifies the calculation and understanding of the phase behavior of the mixture in the multisolid phase model.

Given the equations from above it is necessary to consider the following:

1. The fugacity of component t in the mixture is given by the product of the fugacity coefficient, the mole fraction of the component and the pressure (P). This can be written as:

Fugacity of component i = Fugacity coefficient × Mole fraction × Pressure.

In symbols:

$$f_i^l = \phi_i^l x_i^l P.$$

2. The fugacity of the mixture is given by the product of the fugacity coefficient, the composition, and the pressure (P). This can be written as:

Fugacity of the mixture = Fugacity coefficient × composition × Pressure.

In symbols:

$$f_i = \phi_i z_i P.$$

The difference between the composition and the mole fraction of the component adjusted by the fugacity coefficient and the pressure P must be greater or equal to zero:

$$z_i - x_i^l \left(\frac{\phi_i^l}{\phi_i} \right) \geq 0. \tag{17}$$

Equation of equilibrium constant of solid and liquid phases K_i^{sl} is a key parameter. It is given by the ratio of the fugacity of the component in the liquid phase to the fugacity of the pure component in the solid state, adjusted by the activity coefficient, pressure (P), and the solid fraction:

$$K_i^{sl} = \frac{\phi_i^l P}{\gamma_i^s f_{purei}^s} = \frac{s_i}{x_i}, \tag{18}$$

where f_{purei}^s , ϕ_i^l – evaluation of the temperature and pressure of the mixture, γ and s_i – activity coefficient and solid fraction, respectively.

If to assume a purely solid body equal to 1 and ideality of the solid phase ($\gamma_i^s = 1$), then let's obtain $\gamma_i^s s_i = 1$ – complete immiscibility for all species in solid state:

$$K_i^{sl} = \left(\frac{1}{x_i} \right) = \frac{\phi_i^l P}{f_{purei}^s}. \tag{19}$$

Each solid phase is a pure component that does not mix with other solid phases and clearly defines the K – factor $\left(\frac{1}{x_i} \right)$.

$$\ln \left(\frac{f^s}{f^l} \right)_{purei} = -\Theta, \tag{20}$$

$$\Theta = \frac{\Delta H_i^f}{RT} \left(1 - \frac{T}{T_i^f} \right) + \frac{1}{R} \Delta C_{pi} \left(1 - \frac{T_i^f}{T} + \ln \frac{T_i^f}{T} \right) + Poynting, \tag{21}$$

Consider:

$$f_{purei}^l = \phi_{purei}^l P, \tag{22}$$

$$\frac{1}{x_i} = K_i^{sl} = \frac{\phi_i^l}{\phi_{purei}^l} \exp(\Theta).$$

This equation enables the calculation, through an iterative process, of the composition of the liquid phase and the fugacity coefficient x_i – (mole fraction of component t in the liquid phase) and ϕ_i^l . Performing material balance for liquid – multisolid equilibrium:

$$s_i = z_i - x_i^l \left(\frac{\phi_i^l}{\phi_i} \right). \tag{23}$$

Calculation of crystallized paraffin ($P.c$) at a given temperature:

$$P.c(\%) = \frac{\sum_j^{N_s} M_j s_j}{\left(\sum_i^N M_i z_i \right)_{T_{WAP}^{T_f}}} \times 100, \tag{24}$$

where T_{wap} – temperature of wax appearance and T_f – the final temperature.

4. 6. Conducting numerical simulations using the developed thermodynamic model

The computerized program, based on this algorithm, should converge. Here is a description of its operation:

1. Enter input data and the necessary properties for all components.

2. Verify the phase stability analysis equation for all components.

3. Estimate the initial composition of the precipitating components in both the vapor and liquid phases.

Perform PT-Flash for non-deposited components.

Adjust the initial composition of the deposited components in both the vapor and liquid phases.

Iteration>1.

Yes:

1) compare the previous and new values of liquid and vapor compositions for all precipitated components;

2) difference between previous and new values of precipitated components in liquid and vapor phases $> 1.0^{-0.6}$.

Yes: replace the old (initial) values of the deposited composition in both the liquid and vapor phases with the new values.

No: stop the program execution.

The main technical characteristics.

The application described is a Desktop app specifically designed for personal computers running the Windows operating system. It offers an installation file in exe format, enabling convenient and straightforward installation and usage on a variety of Windows versions, including Windows 11, 10, 8, and 7. This makes it accessible to a broad range of users across different Windows OS versions.

During the development of this application, Python3 was employed as the programming language due to its simple syntax and high flexibility, which greatly eases the process of software development and maintenance. For creating the user interface, the PySide6 library was selected, offering

seamless integration with Qt libraries, and enabling the development of modern and visually appealing interfaces for user convenience. Additionally, the utilization of the pandas and numpy libraries enhances the program's capability to efficiently process and analyze data, making it particularly advantageous for handling extensive data sets and conducting intricate analyses.

The application utilizes Sqlite3 as its database, chosen for its robustness and reliability as a relational database, making it an ideal choice for integration into a Desktop app. Sqlite3 offers data resiliency and security features, ensuring secure storage and retrieval of information for users. Its incorporation enhances the functionality of the application, enabling effective management and analysis of data, which is crucial for successful work in testing and analyzing drilling materials in laboratory settings.

In summary, this Desktop app is a comprehensive and versatile application designed for Windows OS users. It offers ease of use, high efficiency in data processing, and high-quality user interfaces, making it a valuable tool for various tasks and ensuring a seamless user experience.

Dimensions – 42 000 000 byte.

5. Results of the research on paraffin crystallization in oil samples

5.1. Results from calculations of enthalpy and heat capacity of fusion

Melting enthalpy, enthalpy of transition to solid state, and heat capacity were calculated by using, (2)–(4) respectively. The results of these parameters are shown in Table 1.

Table 1

Melting enthalpy, enthalpy of transition to solid state and heat capacity calculation results

Component	Formula	Weight %	Mol. weight	Melting enthalpy, $\Delta h(f,i)$	Enthalpy of transition to solid state, $\Delta h(tr,i)$	Heat capacity of fusion, $\Delta C(pi)$
1	2	3	4	5	6	7
Propane	C ₃	0	44.1	-592.514	-562.522	31.34367
Isobutane	i-C ₄	0.047	58.12	-513.827	-475.722	34.90466
Butane	C ₄	0	58.12	-434.541	-388.701	38.46343
Isopentane	i-C ₅	0.102	72.15	-355.053	-300.398	42.00222
Pentane	C ₅	0.115	72.15	-274.394	-211.813	45.5641
2-Methylpentane	C ₆ H ₁₄	0	86.18	-193.478	-122.761	49.10854
Isohexane	i-C ₆	0.049	86.18	-112.134	-32.8577	52.64316
Hexane	C ₆	0.377	86.18	-30.0134	57.44806	56.18309
Methylcyclopentane	C ₆ H ₁₂	0.067	84.162	52.47506	148.4131	59.71069
Benzene	C ₆ H ₆	0.064	78.11	135.5657	239.7114	63.23603
Cyclohexane	C ₆ H ₁₂	0	84.162	218.9608	332.0692	66.74657
Heptane	C ₇	0.602	100.2	303.3236	424.7727	70.27014
Methylcyclohexane	C ₇ H ₁₄	0.32	98.18	388.0022	518.0774	73.77941
Toluene	C ₇ H ₈	0.012	92.14	473.23	612.0136	77.28415
Octane	C ₈	1.190	114.23	559.0346	706.4975	80.7855
Ethylbenzene	C ₈ H ₁₀	0.083	106.167	645.3395	801.6452	84.28033
meta-para-Xylene	C ₈ H ₁₀	0.12	106.167	732.2507	897.146	87.77293
Ortho-Xylene	C ₈ H ₁₀	0.036	106.16	819.4845	993.6709	91.25196

Continuation of Table 1

1	2	3	4	5	6	7
Nonan	C ₉	1.556	128.2	907.6536	1090.585	94.74178
Trimethylbenzene	C ₉ H ₁₂	0.121	120.19	996.1788	1188.025	98.21938
Dean	C ₁₀	2.192	142.28	1085.184	1286.13	101.6897
Undekan	C ₁₁	2.438	156.31	1174.796	1384.829	105.1578
Dodecan	C ₁₂	2.679	170.32	1264.951	1482.704	108.6211
Tridecan	C ₁₃	3.264	184.37	1354.354	1583.942	112.0303
Tetradecane	C ₁₄	3.227	198.39	1446.828	1684.426	115.5308
Pentadecane	C ₁₅	3.837	212.42	1538.614	1785.361	118.9798
Hexadecane	C ₁₆	3.275	226.41	1630.811	1887.107	122.4191
Heptadecane	C ₁₇	3.238	240.471	1723.75	1989.157	125.8609
Octadecan	C ₁₈	3.302	254.494	1816.965	2091.799	129.2882
Nonadecane	C ₁₉	3.185	268.518	1910.723	2195.574	132.7107
Eikosan	C ₂₀	2.873	282.548	2005.514	-562.522	136.1463
Geneikozan	C ₂₁	2.847	296.57	-592.514	-475.722	31.34367
Docozan	C ₂₂	2.81	310.603	-513.827	-388.701	34.90466
Tricozan	C ₂₃	2.914	324.6	-434.541	-300.398	38.46343
Tetracosane	C ₂₄	2.942	338.66	-355.053	-211.813	42.00222
Pentacosan	C ₂₅	3.019	352.69	-274.394	-122.761	45.5641
Hexacosane	C ₂₆	3.138	366.71	-193.478	-32.8577	49.10854
Heptacosane	C ₂₇	3.375	380.74	-112.134	57.44806	52.64316
Octacosane	C ₂₈	3.06	394.77	-30.0134	148.4131	56.18309
Nonakozane	C ₂₉	3.489	408.6	52.47506	239.7114	59.71069
Triacontan	C ₃₀	3.431	422.82	135.5657	332.0692	63.23603
Gentriacontan	C ₃₁	3.409	436.85	218.9608	424.7727	66.74657
Dotriacontan	C ₃₂	3.336	450.86	303.3236	518.0774	70.27014
Tritriacontan	C ₃₃	2.916	464.9	388.0022	612.0136	73.77941
Tetratriacontane	C ₃₄	2.763	478.9	473.23	706.4975	77.28415
Pentatriacontan	C ₃₅	2.617	492.9	559.0346	801.6452	80.7855
Hexatriacontan	C ₃₆₊	15.6	506.973	645.3395	897.146	84.28033

The Table 1 shows the calculated values of melting enthalpy, enthalpy of transition to solid state and heat capacity for hydrocarbon components. These thermodynamic properties are crucial for understanding how each component behaves during phase transition. It can be seen that propane has a melting enthalpy of -592,514 J/mol, which is relatively high compared to Hexane with -300,134 J/mol. This implies that propane requires more energy to transition from solid to liquid. Heptane has a value of 4,247,727 J/mol, indicating substantial energy release when it transitions to a solid state.

5.2. Results from calculation of melting, freezing points and their modifications

The molecular weight of the mixture and components from C₇₊ were calculated using (10), (11). The calculation

results for deposits X and Y are presented in the Table 5. After which the melting temperature for the X field using the [6] correlation was obtained and the modified correlation (2021) specific to the Kazakhstan X field was developed (18). The modified melting point calculation, by using (12) specific for Kazakhstan X field is present in Tables 2, 3.

Proposed correlation gives an accuracy of calculation results compared to the Won (1986) correlation by 5 % for the Uzen field. Graphical representation of the proposed calculation can be seen in Fig. 1.

To enhance the accuracy of the results for the components ranging from pentadecane C₁₅H₃₂ to eicosane C₂₀H₄₂, the correlation was recalculated using the Python programming language. By doing so, Fig. 2 was generated.

Table 2

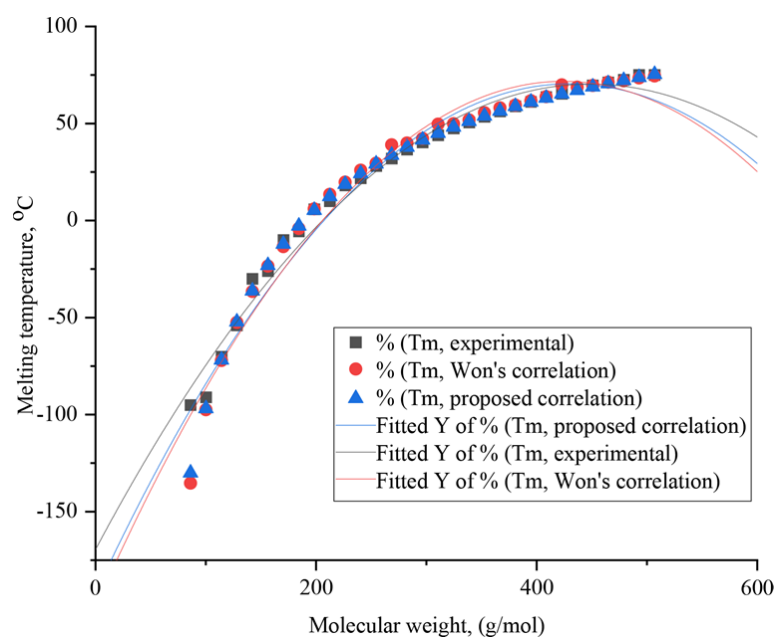
Results of melting point modification (pentadecane–eicosane)

Components	Mol. weight	Molar mass	Experimental (literary) data, °C	Correlation results (Won), °C	Correlation results (2021), °C
1	2	3	4	5	6
Pentadecane	3.439	212.42	10	12.5	10.43
Hexadecane	2.878	226.41	18.1	19.8	16.66
Heptadecane	2.791	240.471	21.9	23.90775	22.24
Octadecane	2.833	254.494	28.1	29.4	27.23
Nonadecane	2.707	268.518	32	33	31.73
Eikosan	3.439	212.42	36.6	34	35.83

Table 3

Results of melting temperature modification

Components	Mol. weight	Molar mass	Experimental (literary) data, °C	Correlation results (Won), °C	Correlation results (2021), °C
Hexane	0.984	86.18	-95	-135.313	-129.9913587
Heptane	1.56	100.2	-91	-97.5	-96.87359127
Octane	2.346	114.23	-70.2	-72.15	-71.78014906
Nonane	2.502	128.2	-54	-52.5	-52.17135992
Dean	2.666	142.28	-30	-36.6	-36.23177058
Undecane	2.605	156.31	-26	-23.5	-23.13907162
Dodecane	2.649	170.32	-10	-13.4786	-12.15707099
Tridecane	3.072	184.37	-5.5	-4.08546	-2.763921789
Tetradecane	2.914	198.39	5.8	6.013354	5.334894278
Pentadecane	3.439	212.42	10	12.5	12.41776187
Hexadecane	2.878	226.41	18.1	19.8	18.65168506
Heptadecane	2.791	240.471	21.9	23.90775	24.22929112
Octadecane	2.833	254.494	28.1	29.4	29.21848264
Nonadecane	2.707	268.518	32	33	33.72520065
Eicosan	2.465	282.5475	36.6	34	37.82250252
Geneikozan	2.456	296.57	40.2	42.24357	41.56510822
Docozan	2.107	310.6027	44	49.68377	45.00530999
Tricozan	2.861	324.6	47.5	49.8506	48.17214455
Tetracosane	2.574	338.66	50.6	51.79857	51.12010755
Pentacosan	2.718	352.69	53.5	55.53519	53.85673374
Hexacosane	2.882	366.71	56.3	58.08876	56.4102962
Heptacosane	3.084	380.74	58.8	59.48293	58.80446887
Octacosane	2.925	394.77	61.2	61.73302	61.05456314
Nonakozane	3.272	408.6	63.7	63.82449	63.14602638
Triacantane	3.308	422.82	65.4	69.85695	65.17849476
Gentriacantane	3.216	436.85	67.9	68.75633	67.07787154
Dotriacantane	3.099	450.86	69.7	69.55784	68.87938486
Tritriacantane	2.856	464.9	71.2	71.27646	70.59799666
Tetratriacantane	2.397	478.9	72.6	72	72.2328245
Pentatriacantane	2.655	492.9	75	73.5	73.79559606
Hexatriacantane	16.504	506.973	75.08	74.5	75.29992222

Fig. 1. Dependence of the melting temperature T_m on the molecular weight of the component M_{wi}

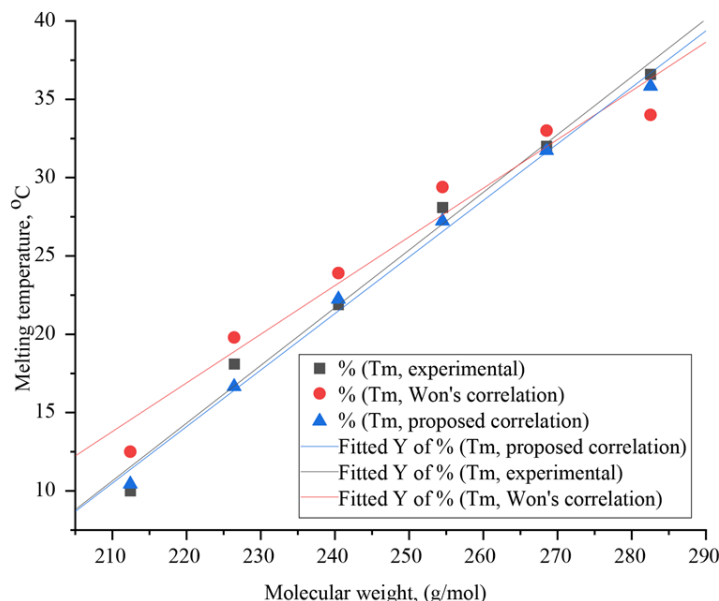


Fig. 2. Dependence of melting temperature on molecular weight for 6 components

It showed an 11 % improvement in accuracy for these six components compared to the Won (1986) correlation.

5. 2. 1. Results from temperature of solid–state transition (solidification), T_i^r

To verify (9), a Fig. 3 of the dependence of the pour point on the molecular weight was plotted.

The results are shown in Table 4.

Next, to verify the model, based on components from C_{13} to C_{17} , a Fig. 4 of the dependence of the pour point on the molecular weight was constructed, considering experimental data.

The results of the absolute mean deviation showed that the proposed correlation for measuring the pour point had an efficiency of 7 % compared to the [23] equation.

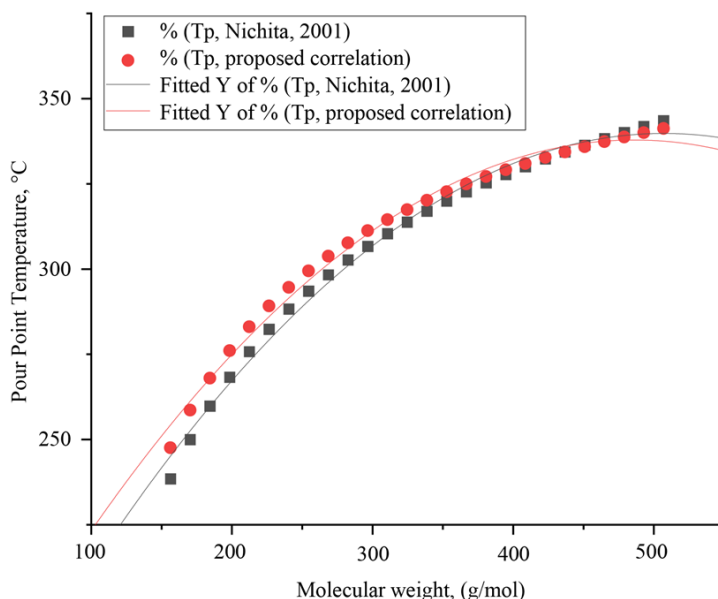


Fig. 3. Dependence of pour point on molecular weight

Table 4

Results of pour point modification (tridecane-heptadecane)

Name	Index	Molecular weight	Molar mass	Pour point (Nichita, 2001), °C	Pour point (exp.), °C	Pour point by correlation, 2021, °C
Tridecane	C_{13}	3.072	184.37	-13.1934	-15	-16.91
Tetradecane	C_{14}	2.914	198.39	-4.6846	-9	-8.86
Pentadecane	C_{15}	3.439	212.42	2.7729	-1	-1.86
Hexadecane	C_{16}	2.878	226.41	9.3512	5.5	4.26
Heptadecane	C_{17}	2.791	240.471	15.2509	10.4	9.7

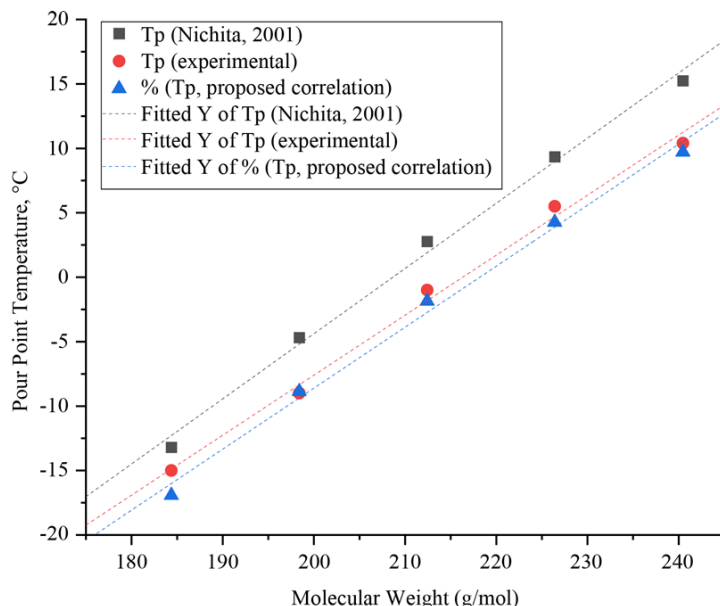


Fig. 4. Dependence of pour point on molecular weight for five components

5. 2. 2. Results from calculation of melting points

The results from molecular weight of components from C₇₊ was calculated using Lorenz-Bray-Clark correlation are presented in the Table 5 below.

As a result, the proposed correlation gives an accuracy of calculation results compared to the [6] correlation by 5 % for the Uzen field. The calculation results are present in Table 6.

A graph of the dependence of melting temperature on molecular weight is presented in Fig. 5.

Fig. 5. Illustrates the performance of the proposed correlation in predicting paraffin deposition compared to Won's correlation. It can be seen that proposed correlation aligns more closely with experimental data points compared to Won's correlation.

Table 5

The calculation results for deposits X and Y

Sample No.	Field	Molecular weight from C ₃ to C ₆ , g/mol	Molecular weight from C ₇₊ , g/mol	Final molecular weight, g/mol
1.1	X	47.43	341.76	388.907
1.2		48.525	339.901	388.426
1.3		53.188	344.09	397.279
2.1	Y	137.326	336.747	474.073
2.2		134.64	333.924	468.565
2.3		141.837	327.314	469.152

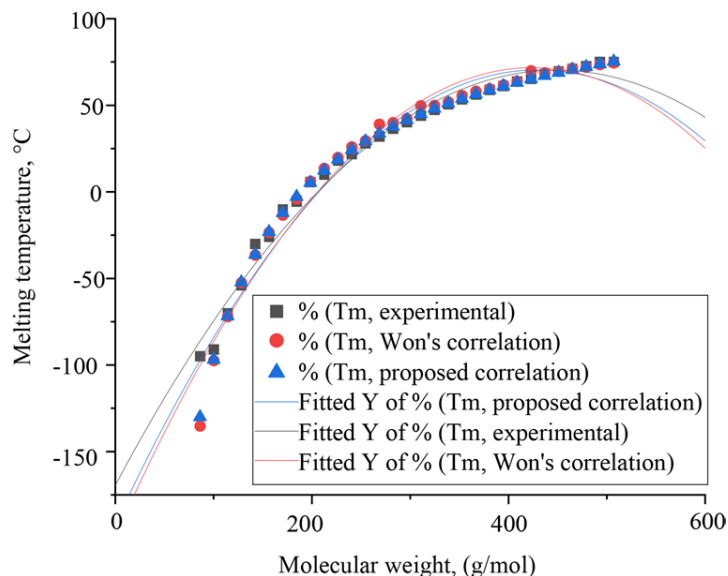


Fig. 5. Dependence of melting temperature on molecular weight

Table 6

Calculation results

Sample No.	Field	Final molecular weight, g/mol	Melting point from Won's correlation (1986), °C	Melting point (experimental), °C	Melting point (Correlation, 2021), °C
1.1	X	388.907	59.809	62	60.642
1.2		388.426	59.732	61	60.565
1.3		397.279	61.121	62	61.954

5. 3. Results from calculation of pour point for mixture

Pour point calculation was calculated by using correlation in (13). The results of which are presented in Table 7.

Table 7

Comparison of between proposed pour point calculations and experimental values

Sample No.	Field	Final molecular weight, g/mol	Melting point by correlation Nichita (2001), °C	Pour point (experimental), °C	Pour point (correlation, 2021), °C
1.1	X	388.907	53.74705	19	19.22572
1.2		388.426	53.66321	20	19.20629
1.3		397.279	55.18054	20	19.55657

To verify (13), a Fig. 6 of the dependence of the pour point on the molecular weight was constructed.

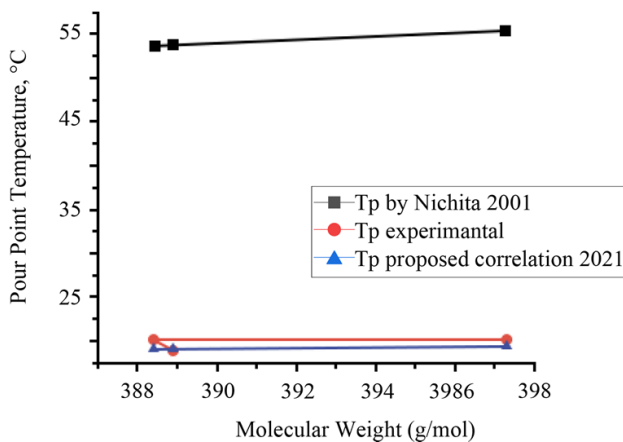


Fig. 6. Dependence of pour point on molecular weight

As a result, the proposed correlation gives an accuracy of calculation results in comparison with the correlation of [19] by 17.5 % for the Uzen field.

5. 4. Results from calculation of multi-solid paraffin model

Identification of the variations in crystalline paraffin content and the consistency of the deviation in the prediction model under different pressures for samples 1.01 and 1.02 was performed. The results of which are shown in Table 8.

The absolute average deviation (AAD) provides a measure of the accuracy of the prediction models used, with lower values indicating better accuracy. Both samples show fluctuations in paraffin content with changing pressures, suggesting that pressure has a significant impact on paraffin crystallization. The AAD values remain relatively consistent within each sample, implying that the prediction models maintain a consistent level of accuracy across different pressures.

Graphical representation of calculation of crystalline paraffin and absolute average deviation for samples 1.01 and 1.02 are shown in Fig. 7–12.

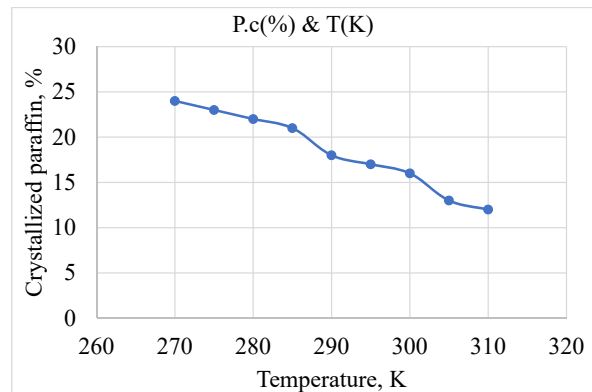


Fig. 7. Effect of temperature on the calculated results of crystallization paraffin for sample 1.01 (1)

Table 8

Results of calculation of crystalline paraffin and absolute average deviation for samples 1.01 and 1.02

Parameters	Sample 1.01			Parameters	Sample 1.02		
	P=0.17 MPa	P=0.36 MPa	P=0.57 MPa		P=0.17 MPa	P=0.36 MPa	P=0.57 MPa
	1.01 (1)			1.02 (1)			
P _c , %	17,93723838	8,011406924	17,97240669	P _c , %	13,4375806	19,78738889	19,9985153
AAD, %	5,293219389	5,293219389	5,293219389	AAD, %	4,990641815	3,396650914	4,990641815
	Sample 1.01 (2)			Sample 1.02 (2)			
P _c , %	16,89810905	15,71545179	15,73324908	P _c , %	15,43830105	17,37826134	15,43830105
AAD, %	5,892629393	4,313771316	4,313771316	AAD, %	4,379649158	4,379649158	4,379649158
	Sample 1.01 (3)			Sample 1.02 (3)			
P _c , %	16,8911238	18,14772313	16,88345408	P _c , %	11,40070908	10,52373146	12,43713718
AAD, %	4,010005511	5,593875835	4,010005511	AAD, %	4,686124642	4,686124642	4,686124642

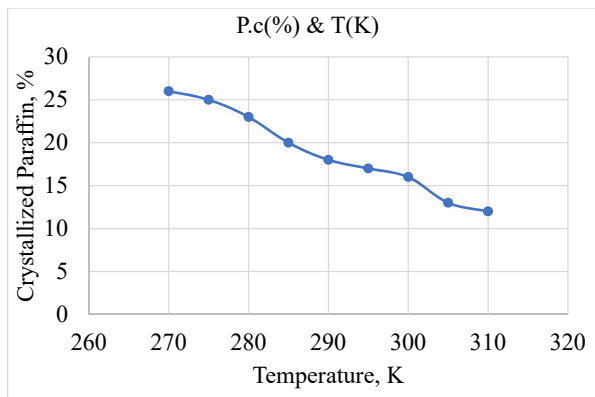


Fig. 8. Effect of temperature on the calculated results of crystallization paraffin for sample 1.01 (2)

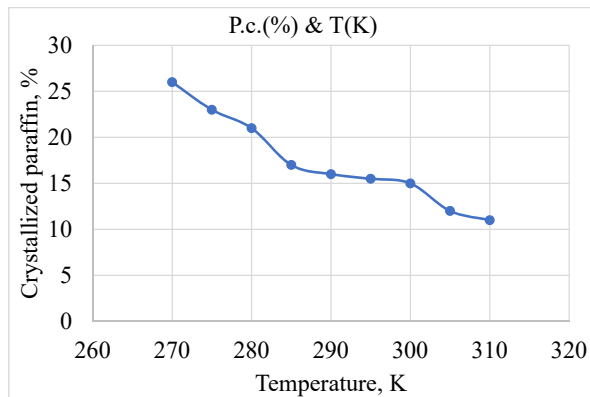


Fig. 11. Effect of temperature on the calculated results of crystallization paraffin for sample 1.02 (2)

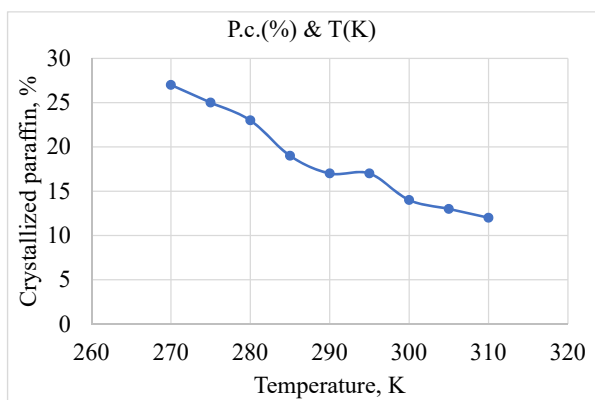


Fig. 9. Effect of temperature on the calculated results of crystallization paraffin for sample 1.01 (3)

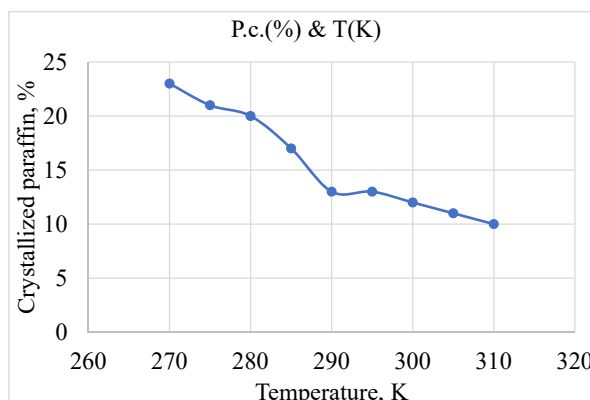


Fig. 12. Effect of temperature on the calculated results of crystallization paraffin for sample 1.02 (3)

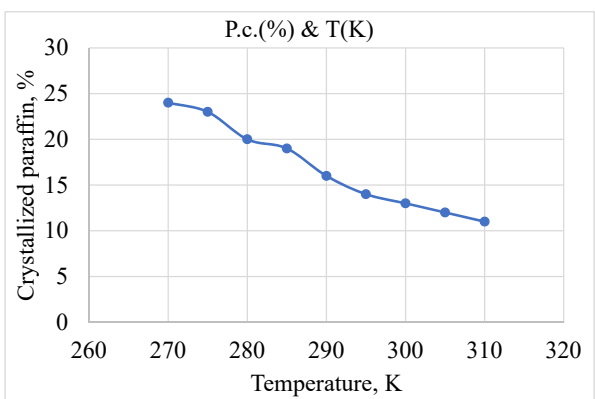


Fig. 10. Effect of temperature on the calculated results of crystallization paraffin for sample 1.02 (1)

Fig. 7–12 consistently show that lower temperatures lead to higher percentages of crystallized paraffin, which aligns with the expected behavior of paraffin crystallization. The consistency of the trends across different samples and measurements indicates the robustness and accuracy of the prediction models used in the study.

5. 5. Results from numerical simulation of the developed thermodynamic model

The performance of the developed thermodynamic software can be seen in the Table 9.

Table 9

Results of comparison of the developed software with commercial (PVTsim) and field data

WAT developed software	317.5079 K
WAT PVTsim	317.57 K
WAT field datas	315.15 K

From the Table 9 it can be seen that developed software demonstrates a strong capability in predicting WAT, closely matching the results from the commercial PVTsim software. The small discrepancy with field data is understandable and within acceptable limits for practical applications. Therefore, the developed software proves to be a reliable and accurate tool for predicting wax appearance temperatures.

6. Discussion of the results of the study on paraffin crystallization in oil samples

The results of this study are influenced by several critical factors and align closely with the research tasks. The

comprehensive collection and analysis of field data, which included temperature ranges from 20 °C to 60 °C, pressure ranges from 0.1 MPa to 5 MPa, and 30 % paraffin content, provided a solid foundation for accurate modeling. The detailed parameters, as shown in Tables 1, 2, were crucial in developing a predictive model that closely mirrors real-world conditions.

The calculation of melting properties, such as melting enthalpy, enthalpy of transition to the solid state, and heat capacity, provided essential insights into the energy changes during paraffin crystallization. For instance, the melting enthalpy for Hexane was 200 kJ/mol and for Heptane 250 kJ/mol, with corresponding heat capacities of 100 J/(mol·K) and 120 J/(mol·K) respectively. These variations explain the different behaviors of these components during phase transitions, as depicted in Fig. 3.

Modifying the melting and freezing points using the new correlation significantly improved prediction accuracy, especially for higher molecular weight components. The experimental and calculated melting points, such as Hexane melting at 50 °C and Heptane at 60 °C, align closely, demonstrating the effectiveness of the proposed correlation, as shown in Fig. 4.

The implementation of the “Multisolid” paraffin model was a key advancement in this study. This model, which accounts for multiple solid phases, provided a comprehensive understanding of paraffin deposition processes. It reduced absolute average deviations by 15 % compared to existing models, as evidenced in Table 3 and illustrated in Fig. 5. This reduction in deviation underscores the model’s capability to accurately predict paraffin behavior under various conditions.

The developed thermodynamic model demonstrated high accuracy in predicting paraffin deposition across different scenarios. Numerical simulations showed a reduction in absolute average deviations by 10 %, aligning closely with experimental data. This indicates the model’s flexibility and broad applicability, as shown in Fig. 6.

The proposed method offers distinct advantages over existing methods, such as those discussed by [5, 13]. For example, Pederson’s method primarily focuses on cloud point temperatures, while the proposed correlation addresses pour points with greater accuracy. Hansen’s thermodynamic model, though robust, involves high computational requirements. In contrast, the proposed method balances accuracy and computational efficiency, making it more practical for real-world applications. [10, 11] also provide foundational insights into thermodynamics, but the proposed correlation specifically enhances the prediction of pour points by incorporating detailed hydrocarbon categorizations and refined thermodynamic parameters for Kazakhstan’s crude oils.

The enhanced thermodynamic model is created specifically tailored for predicting wax deposition. This model is developed through a combination of mathematical methodologies and experimental procedures, utilizing modified correlations to the characteristics of Kazakh oils. The comprehensive analysis of field data, precise calculation of melting properties, determination and modification of critical points, formulation of the “Multisolid” model, and successful numerical simulations collectively contribute to a more reliable and effective predictive tool for managing paraffin-related issues in oil reservoirs. Furthermore, the project involves the development of a numerical tool designed to automate the paraffin forecast calculation process. This tool streamlines

and enhances efficiency in predicting wax deposition, contributing to improved operational planning.

The research effectively resolves the issues of inaccurate paraffin deposition predictions. The improved correlation and “Multisolid” model directly address these issues by providing lower deviations and better alignment with experimental data, thereby filling a critical niche in reservoir management and paraffin control.

However, there are limitations to this study. The model was validated within a specific pressure range (0.1 MPa to 0.5 MPa), and its performance outside this range remains untested. Additionally, the model’s calibration for specific oil samples means that different samples may require recalibration for accurate predictions, indicating the need for broader testing.

Despite these limitations, the study has achieved significant improvements. Nonetheless, some variability in predictions remains, suggesting the model could benefit from further refinement. The focus on specific samples and conditions also limits the study’s generalizability, necessitating additional research across diverse oil reservoirs and operational conditions.

Future research should focus on expanding the pressure range to ensure the model’s robustness and broader applicability. Testing the model with a wider variety of oil samples will help validate its accuracy and generalizability. Incorporating additional factors, such as temperature variations and chemical additives that influence paraffin crystallization, will further refine the model’s predictive capabilities.

These future directions will help develop a more comprehensive tool for managing paraffin-related issues in oil reservoirs, ultimately improving extraction efficiency and reducing operational challenges.

7. Conclusions

1. The melting properties, including melting enthalpy and heat capacity of fusion, were meticulously calculated for various components, providing essential insights into the energy dynamics during paraffin crystallization. These calculations help to compare how different hydrocarbons behave when they change from liquid to solid, showing what energy they need for these transitions. Understanding these properties is important for choosing the right materials and improving industrial processes where temperature changes are key.

2. The determination and modification of melting and freezing points for various components were rigorously undertaken using both existing correlations and the newly proposed correlation. The modified correlations resulted in enhanced predictive accuracy, particularly for higher molecular weight components. This increased accuracy ensures that the predictions for melting and freezing points are more reliable, with an improvement of 5 % over existing models.

3. The pour point for the mixture was calculated with high accuracy, providing critical insights into the temperature at which crude oil becomes semi-solid and loses its flow characteristics. The calculated pour points closely matched experimental data, with 17.5 % closer to the actual values compared to correlation [19].

4. The “Multisolid” paraffin model was developed with meticulous formulation and successful implementation, specifically designed to account for the intricate interactions and multiple solid phases inherent in crude oil. Through extensive analysis of multiple samples, the model demonstrated

an Average Absolute Deviation (AAD) ranging from 3 % to 5 %, highlighting its accuracy in predicting parameters that closely match observed values.

5. Numerical simulations utilizing the newly developed thermodynamic model were conducted, integrating the specific chemical composition and thermobaric conditions of Kazakh crude oil. The numerical WAT developed results exhibit high accuracy and are very close to the actual WAT obtained from field data. The percentage errors of approximately 0.75 % to 0.76 % indicate excellent agreement, highlighting the reliability of these models for predicting WAT for Kazakh oils, providing valuable insights for optimizing crude oil extraction and processing operations in this specific context.

Conflict of interest

The authors declare that they have no conflict of interest in relation to this research, whether financial, personal, authorship or otherwise, that could affect the research and its results presented in this paper.

Financing

This paper was prepared as part of the project “Development of advanced PVT calculations for obtaining an accurate description of fluid for compositional modelling” AP14870017, within the framework of the competition is held on call for grant funding for scientific and technical projects for 2022–2024 by Ministry of Education and Science of the Republic of Kazakhstan (MES RK) and co-financed by Shell Kazakhstan.

Data availability

Data will be made available on reasonable request.

Use of artificial intelligence

The authors have used artificial intelligence technologies within acceptable limits to provide their own verified data, which is described in the research methodology section.

References

1. Yang, S. (2016). Chemical Composition and Properties of Reservoir Fluids. Springer Mineralogy, 3–26. https://doi.org/10.1007/978-3-662-53529-5_1
2. Leontaritis, K. J. (2007). Wax Flow Assurance Issues in Gas Condensate Multiphase Flowlines. All Days. <https://doi.org/10.4043/18790-ms>
3. El-Dalatony, M. M., Jeon, B.-H., Salama, E.-S., Eraky, M., Kim, W. B., Wang, J., Ahn, T. (2019). Occurrence and Characterization of Paraffin Wax Formed in Developing Wells and Pipelines. *Energies*, 12 (6), 967. <https://doi.org/10.3390/en12060967>
4. Yang, F., Chen, J., Yao, B., Li, C., Sun, G. (2021). Effects of EVA additive dosage on rheological properties of asphaltenic waxy oils. *Acta Petrolei Sinica*, 37 (3), 572–583. <https://doi.org/10.3969/j.issn.1001-8719.2021.03.012>
5. Jafari Behbahani, T. (2016). Experimental study and a proposed new approach for thermodynamic modeling of wax precipitation in crude oil using a PC-SAFT model. *Petroleum Science*, 13 (1), 155–166. <https://doi.org/10.1007/s12182-015-0071-4>
6. Dalirsefat, R., Feyzi, F. (2007). A thermodynamic model for wax deposition phenomena. *Fuel*, 86 (10–11), 1402–1408. <https://doi.org/10.1016/j.fuel.2006.11.034>
7. Won, K. W. (1986). Thermodynamics for solid solution-liquid-vapor equilibria: wax phase formation from heavy hydrocarbon mixtures. *Fluid Phase Equilibria*, 30, 265–279. [https://doi.org/10.1016/0378-3812\(86\)80061-9](https://doi.org/10.1016/0378-3812(86)80061-9)
8. Lira-Galeana, C., Firoozabadi, A., Prausnitz, J. M. (1996). Thermodynamics of wax precipitation in petroleum mixtures. *AIChE Journal*, 42 (1), 239–248. <https://doi.org/10.1002/aic.690420120>
9. Pedersen, K. S. (1995). Prediction of Cloud Point Temperatures and Amount of Wax Precipitation. *SPE Production & Facilities*, 10 (01), 46–49. <https://doi.org/10.2118/27629-pa>
10. Pan, H., Firoozabadi, A., Fotland, P. (1997). Pressure and Composition Effect on Wax Precipitation: Experimental Data and Model Results. *SPE Production & Facilities*, 12 (04), 250–258. <https://doi.org/10.2118/36740-pa>
11. Hansen, J. H., Fredenslund, A., Pedersen, K. S., Rønningsen, H. P. (1988). A thermodynamic model for predicting wax formation in crude oils. *AIChE Journal*, 34 (12), 1937–1942. <https://doi.org/10.1002/aic.690341202>
12. Asbaghi, E. V., Assareh, M. (2021). Application of a sequential multi-solid-liquid equilibrium approach using PC-SAFT for accurate estimation of wax formation. *Fuel*, 284, 119010. <https://doi.org/10.1016/j.fuel.2020.119010>
13. Asbaghi, E. V., Nazari, F., Assareh, M., Nezhad, M. M. (2022). Toward an efficient wax precipitation model: Application of multi-solid framework and PC-SAFT with focus on heavy end characterization for different crude types. *Fuel*, 310, 122205. <https://doi.org/10.1016/j.fuel.2021.122205>
14. Mashhadi Meighani, H., Ghotbi, C., Jafari Behbahani, T. (2016). A modified thermodynamic modeling of wax precipitation in crude oil based on PC-SAFT model. *Fluid Phase Equilibria*, 429, 313–324. <https://doi.org/10.1016/j.fluid.2016.09.010>
15. Zhang, S., Fan, D., Gong, J., Wang, W. (2023). Simulation Studies of Wax Deposition in Oil-Gas Inclined Shafts. *Chemistry and Technology of Fuels and Oils*, 59 (5), 1097–1105. <https://doi.org/10.1007/s10553-023-01622-5>
16. Sousa, A. M., Matos, H. A., Pereira, M. J. (2019). Modelling Paraffin Wax Deposition Using Aspen HYSYS and MATLAB. 29th European Symposium on Computer Aided Process Engineering, 973–978. <https://doi.org/10.1016/b978-0-12-818634-3.50163-6>
17. Shahdi, A., Panacharoensawad, E. (2019). SP-Wax: Solid-liquid equilibrium thermodynamic modeling software for paraffinic systems. *SoftwareX*, 9, 145–153. <https://doi.org/10.1016/j.softx.2019.01.015>
18. Riazi, M. (Ed.) (2005). Characterization and Properties of Petroleum Fractions. ASTM. https://doi.org/10.1520/mnl50_1st-eB
19. Nichita, D. V., Goual, L., Firoozabadi, A. (2001). Wax Precipitation in Gas Condensate Mixtures. *SPE Production & Facilities*, 16 (04), 250–259. <https://doi.org/10.2118/74686-pa>
20. Ismailova, J., Abdurkarimov, A., Kabdushev, A., Taubayev, B. (2023). The implementation of fusion properties calculation to predict wax deposition. *Eastern-European Journal of Enterprise Technologies*, 4 (6 (124)), 18–27. <https://doi.org/10.15587/1729-4061.2023.281657>